Model Calculations of Solar Spectral Irradiance in the 3.7 μm Band for Earth Remote Sensing Applications

Steven Platnick and Juan M. Fontenla

For publication in

Journal of Applied Meteorology and Climatology

Submitted: 31 August 2006

Revised: 31 January 2007

Corresponding author addresses:

S. Platnick, Laboratory for Atmospheres, NASA Goddard Space Flight Center, Greenbelt, MD 20771 USA, steven.platnick@nasa.gov.

J. M Fontenla, Laboratory for Atmospheric and Space Physics, University of Colorado, Boulder, CO 80303 USA, juan.fontenla@lasp.colorado.edu.

ABSTRACT

Since the launch of the first Advanced Very High Resolution Radiometer (AVHRR) instrument aboard TIROS-N, measurements in the 3.7 μm atmospheric window have been exploited for use in cloud detection and screening, cloud thermodynamic phase and surface snow/ice discrimination, and quantitative cloud particle size retrievals. The utility of the band has led to the incorporation of similar channels on a number of existing satellite imagers and future operational imagers. Daytime observations in the band include both reflected solar and thermal emission energy. Since 3.7 μm channels are calibrated to a radiance scale (via onboard blackbodies), knowledge of the top-of-atmosphere solar irradiance in the spectral region is required to infer reflectance. Despite the ubiquity of 3.7 μm channels, absolute solar spectral irradiance data comes from either a single measurement campaign (Thekaekara et al. 1969) or synthetic spectra.

In this study, we compare historical 3.7 μm band spectral irradiance data sets with the recent semi-empirical solar model of the quiet-Sun by Fontenla et al. (2006). The model has expected uncertainties of about 2% in the 3.7 μm spectral region. We find that channel-averaged spectral irradiances using the observations reported by Thekaekara et al. are 3.2–4.1% greater than those derived from the Fontenla et al. model for MODIS and AVHRR instrument bandpasses; the Kurucz spectrum (1995), as included in the MODTRAN4 distribution, gives channel-averaged irradiances 1.2–1.5% smaller than the Fontenla model. For the MODIS instrument, these solar irradiance uncertainties result in cloud microphysical retrievals uncertainties comparable with other fundamental reflectance error sources.

I. Introduction

The 3.7 μm atmospheric window was first used in satellite Earth remote sensing with the 1978 launch of the original 4-channel Advanced Very High Resolution Radiometer (AVHRR) instrument aboard the TIROS-N polar orbiter. AVHRR has retained this spectral capability up to the present (currently through the NOAA-18 polar platform, though post NOAA-15 platforms carry the AVHRR/3 version of the instrument which has a single data channel shared by both 3.7 μm and 1.6 μm spectral channels). The main objective in originally flying the channel was reported to be for cloud screening of sea surface temperature observations (Schwalb 1982). Measurements in this window are now routinely used for cloud detection and screening (Saunders and Kriebel 1988; Ackerman et al. 1998; Heidinger et al. 2002); fire detection (Kaufman 1991; Prins and Menzel 1992, Justice et al. 2002); cloud phase and surface snow/ice discrimination (Pavolonis et al. 2005); and quantitative cloud microphysical retrievals (Arking and Childs 1985; Platnick and Twomey 1994; Han et al. 1994; Minnis et al. 1995; Platnick et al. 2003). The usefulness of the band for cloud observations essentially derives from the significant dependence of single scattering albedo on cloud thermodynamic phase and particle size (absorption increases for the ice phase and with particles size), and differences in single scattering albedo (and thereby cloud emissivity) compared to window IR channels. Smaller land surface emissivity compared to window bands also provides contrast. Qualitative overviews of 3.7 μm imagery from AVHRR and its uses for clouds and sea ice discrimination can be found in Scorer (1986, 1989).

The usefulness of the spectral band has led to the incorporation of a 3.7 μm channel on a number of low Earth orbit imagers over the last decade. Examples include the Along-Track Scanning Radiometer (ATSR) on board ERS-1/-2 and

ENVISAT, Visible Infrared Scanner (VIRS) on the TRMM spacecraft (Barnes et al. 2000), Moderate Resolution Imaging Spectroradiometer (MODIS) on the Terra and Aqua spacecrafts (Barnes et al. 1998), and Global Imager (GLI) on Midori-II (ADEOS-II) (Nakajima et al. 1998). On geosynchronous platforms, 3.9 μm channels are available on the new GOES Imager and the Meteosat Second Generation (MSG) Spinning Enhanced Visible and Infrared (SEVIRI) instrument (Aminou 2002). Future operational imagers will continue to fly similar channels for weather and climate applications, including the Visible Infrared Imager Radiometer Suite (VIIRS) on the National Polar-orbiting Operational Satellite System (NPOESS) and NASA's NPOESS Preparatory Project (NPP) (Lee et al. 2006), AVHRR/3 on the European Space Agency MetOp platforms, and the GOES-R Advanced Baseline Imager (ABI) (Schmit et al. 2005). Similar channels have also been included on aircraft imagers (e.g., the MODIS Airborne Simulator flown on NASA's high altitude ER-2 aircraft, King et al. 1996).

Daytime quantitative use of the 3.7 μm band for cloud microphysical retrievals must account for contributions from both reflected solar and thermal emission energy. The observed cloud bidirectional reflectance and emissivity, and not the measured radiance itself, are the fundamental quantities relevant for cloud microphysical retrievals. In this paper, we examine the fundamental uncertainty in the observed 3.7 μm solar reflectance that corresponds to uncertainty in the knowledge of the solar irradiance in this spectral region. The partitioning between solar and emissive radiance in practical cloud retrieval algorithms is not discussed here.

While many modern imagers have onboard solar diffusers to provide a direct reflectance calibration scale for solar spectral channels (e.g., MODIS), these calibration systems do not extend into the 3.7 μm region. A 3.7 μm channel is

calibrated to a radiance scale (via onboard blackbodies) and knowledge of the top-of-atmosphere (TOA) solar irradiance across the channel's spectral bandpass is required to infer reflectance. The observed bidirectional reflectance of an Earth-atmosphere scene is

$$R = \frac{\pi I}{\mu_0 F_0}, \tag{1}$$

where μ_0 is the cosine of the solar zenith angle, I is the satellite measured radiance for the viewing geometry, and F_0 is the TOA solar irradiance. All radiative quantities in Eq. (1) are averages over the spectral bandpass of the instrument, i.e.,

$$\begin{aligned} F_0 &= \frac{\int_{\Delta\lambda} F_0(\lambda)\Phi(\lambda)\,d\lambda}{\int_{\Delta\lambda}\Phi(\lambda)\,d\lambda} \\ I &= \frac{\int_{\Delta\lambda} I(\lambda)\Phi(\lambda)\,d\lambda}{\int_{\Delta\lambda}\Phi(\lambda)\,d\lambda} \\ R &= \frac{\int_{\Delta\lambda} R(\lambda)F_0(\lambda)\Phi(\lambda)\,d\lambda}{\int_{\Delta\lambda} F_0(\lambda)\Phi(\lambda)\,d\lambda} \end{aligned}, \tag{2}$$

where $\Phi(\lambda)$ is the instrument channel spectral response function. The relative uncertainty in reflectance due to uncertainty in the averaged irradiance over the channel can be written as

$$\begin{aligned} \frac{R_2 - R_1}{R_1} &= -\frac{F_{02} - F_{01}}{F_{02}} \\ \frac{\Delta R}{R} &\approx -\frac{\Delta F_0}{F_0} \end{aligned}, \tag{3}$$

with F_{01} and F_{02} representing calculations from two different spectral irradiance datasets. Note the different denominator indexes in the exact expression. As an example, an overestimation in the band-averaged solar irradiance results in an underestimation of reflectance.

Despite the widespread use of 3.7 μm satellite and aircraft measurements, only a single set of observations of absolute TOA spectral irradiance from the entire solar disk has been reported in this spectral region (Thekaekara et al. 1969; Thekaekara 1974). Further, the measurements are at a relatively poor spectral resolution. Here we give an overview of the historical observational data and common synthetic data sets of spectral irradiance in the 3.7 μm band, and compare these data with the new semi-empirical quiet-Sun model from Fontenla el al. (2006). The model's solar atmospheric parameters are adjusted to match available satellite solar spectral irradiance observations; the model explicitly includes the effect of solar activity (both the distribution and radiative effects of sunspots, plages, and networks). Model irradiances in the 3.7 μm spectral region are expected to have uncertainties of about 2%; deviations from quite sun values are found to be less than 0.5%.

While a recent study by Trishchenko (2006) examined differences in AVHRR and GOES imager 3.7 μm band reflected radiance and brightness temperature calculations using four solar irradiance data sets (compiled observational as well as synthetic), our current study includes a critical discussion of the original observational data as well as the new Fontenla et al. (2006) models, with an emphasis on cloud retrieval applications using the MODIS sensor.

Section 2 gives an overview of the existing 3.7 μm band absolute spectral irradiances data sets, in particular, those that have typically been used to convert

radiance measurements to solar reflectances for quantitative cloud microphysical retrievals. Section 3 summarizes the Fontenla et al. (2006) set of models and compares the quiet-Sun spectral irradiance with the historic data sets. The resulting differences in the band-averaged solar irradiance for ten AVHRR instruments (NOAA-7 through NOAA-18) and both MODIS instruments (Terra and Aqua) are given. Relative differences in inferred reflectance using the various irradiance data sets are also given for each instrument. We conclude with a discussion on the impact of solar irradiance uncertainty on cloud microphysical retrievals.

2. Overview of Historical 3.7 μm Spectral Irradiance Data Sets

The only observational absolute spectral irradiance data set covering the 3.7 μm band was obtained during the August 1967 aircraft campaign described by Thekaekara et al. (1969, 1974). Instrument and analysis details of the flights off the coast of California are extensively discussed in Thekaekara et al. (1969) and summarized here.

Measurements were made from the NASA Convair CV-990 aircraft flying at an altitude of 11.5 km. During the six-flight campaign, a variety of total and spectral irradiance measurements were obtained from 12 instruments, only two of which measured spectral irradiance in the 3.7 μm band: a prism monochrometer (operated by Thekaekara et al.) and a Michaelson interferometer. To obtain irradiance over the entire solar disk, the monochrometer used a diffuse incident mirror with radiometric calibration traceable to a standard lamp; corrections were required to account for the additional optical path of sunlight through a sapphire window on the aircraft. The interferometer was calibrated to an onboard blackbody with corrections for detector and instrument emission. A "weighted average" of irradiance from the monochrometer and interferometer

instruments was reported for the 3.7 μm band though no details on the weighting were given. An overall statement of the derived spectral irradiance accuracy was estimated at ±5%. This assessment was not specified as a function of wavelength. Spectral irradiance in the 3.7 μm band was reported at 100 nm resolution. All irradiances were normalized to the average sun-earth distance (1 AU).

Observations were made over a range of solar zenith angles and so corrections for slant path (air mass) as well as the atmospheric path absorption are critical. In the visible portion of the spectrum, air mass corrections derived from the Langley plot method for a single flight day were used to extrapolate observations to zero air mass for all flights (with the implicit assumption that the above-flight level amount of absorbing gases and aerosol did not significantly change during the multi-day observations). Otherwise, it appears that a zero air mass correction was obtained from a weighted average of solar zenith angle observations and ground-based air mass calculations (details on the weighting not described). Atmospheric spectral attenuation calculations are those of Elterman and Toolin (1965) for the U.S. Standard Atmosphere. Table 7-4 in Elterman and Toolin provides optical properties at 3.5 and 4.0 μm; at both wavelengths, the optical thickness between 11 km and TOA is given as zero. Molecular absorption in the 3.7 μm band is now known to be important (primarily CH_4 and N_2O in the short and longer wavelength portions of the band, respectively, along with water vapor absorption throughout the band). We performed our own calculations using the MODTRAN atmospheric transmittance code (Berk et al., 2003) for a Mid-latitude Summer standard atmosphere, an atmospheric path from 11 km to TOA, and an air mass of 2 (air masses over the course of the six CV-990 flights ranged from near-unity to 7). Averaged over 50 nm bandpasses (estimated grating resolution at these wavelengths), the atmospheric path absorptance was 0.024, 0.006,

0.006, 0.040, 0.021 at 3.6, 3.7, 3.8, 3.9, and 4.0 μm, respectively. Though a critical function of air mass, it appears that a significant 2-4% absorption on either side of the 3.7 μm atmospheric window was likely even at CV-990 altitudes, and not accounted for in the analysis.

Absolute radiance measurements in the spectral region include those of Kondratyev et al. (1965), obtained from Mt. Elbrus in the Caucasus mountains (5.6 km altitude) over a two-year period, who reported results for the solar disk center at 3.0, 3.6, and 4.0 μm. Their results were converted to irradiance by Pierce and Allen (1977), along with the radiance measurements of Koutchmy and Peyturaux (1970) from Mt. Louis in the Pyrenees at 3.8 μm and the 31 km altitude balloon measurements of Murcray et al. (1964) at 4.0 and 4.1 μm. However, the solar limb darkening curve(s) used for the Pierce and Allen calculations was not discussed. The derived spectral irradiances for Kondratyev et al. are about 15% smaller than Thekaekara et al. at 3.6 μm; the Koutchmy and Peyturaux derived irradiance is identical with Thekaekara (at 1 $W\text{-}m^{-2}\text{-}\mu m^{-1}$ precision); irradiances for Murcray et al. are 14% smaller than Thekaekara et al. at both wavelengths. Kondratyev et al. give uncertainties of a few percent in the 3.7 μm band, as does Murcray et al. for their 4-5 μm measurements. A summary of these and other historical solar spectral observations is given in Pierce and Allen (1977).

High spectral resolution interferometer observations of solar disk-center radiance covering the mid-wave infrared have also been published. These data include the ATMOS space shuttle experiment Fourier Transform Spectrometer observations (Farmer 1994) and the ground-based Kitt Peak atlas of Livingston and Wallace (1991). However these data were intended for spectroscopic studies and are not absolutely calibrated.

Several compilations of observational and/or modeled solar irradiance spec-

tra are in wide use by the remote sensing community. The World Radiation Center (WRC) Reference Spectrum (Wehrli 1985) adopted by WMO is a compilation from a number of sources. For the present discussion, irradiance in the mid-wave infrared portion of the spectrum comes from Smith and Gottlieb (1974), which is in turn, a compilation of several sources. All data points from Smith and Gottlieb in the 3.7 μm spectral region are from the few Koutchmy and Peyturaux (1970) and Murcray et al. (1964) radiance measurements previously discussed; again, no information is given regarding the limb darkening curves used for the radiance to irradiance conversion in this spectral region. To compensate for the sparse data in this spectral region, Smith & Gottlieb provided the coefficients of a linear fit to a log-log plot of the available data; this means of interpolation is apparently used to provide the 10 nm resolution found in Wehrli.

A data set by Kurucz (1995) was incorporated into the Moderate Spectral Resolution Atmospheric Transmittance (MODTRAN) radiative transfer model along with some later modifications (Berk et al. 2003; see file *DATA/newkur.dat* in the MODTRAN4 distribution). While MODTRAN4 provides options for using other irradiance data sets for various parts of the solar spectrum, the Kurucz quiet-Sun spectrum is the sole data set covering the 3.7 μm spectral region. From the available documentation, the Kurucz spectrum is calculated using a solar atmospheric model from Avrett (that may have been further modified), and lines and atomic data compiled by Kurucz. The *ASTM E-490* solar spectrum (2000), developed for use by the aerospace community, also uses the Kurucz spectra in the 3.7 μm band.

3. New Spectral Irradiance Calculations

With only a single absolute observational irradiance dataset available, and

difficulty and/or lack of information for deriving irradiance uncertainties from the solar radiance observations, it is important to include information available from solar models in assessing the state of the knowledge for this spectral region. Here we give a brief description of calculations using the Fontenla et al. (2006) published set of solar models that were further developed by Fontenla et al. (2006b) and describe the relevant atomic and molecular data for computing the spectrum in the 3.7 μm band. We then compare our results with the historical datasets described in Section 2. The newly computed quiet-Sun spectrum from Fontenla et al., as implemented in the Solar Radiation Physical Modeling (SRPM) system (described below) and covering a spectral range from the UV to centimetric radio wavelengths, is planned for inclusion in the upcoming MODTRAN5 release (G. Anderson, private communication).

a. Overview of the model

The solar irradiance spectrum is calculated from the model atmospheres of solar surface features reported by Fontenla el al. (2006). Model C from that dataset is used in this study. The model consists of solar atmospheric parameters as a function of height that are based on earlier work and constrained by comparisons with available ground and space observations of line profiles and continuum of the emitted radiance at visible and infrared wavelengths. Among these observations, absolutely calibrated space-based observations of the solar spectral irradiance in the visible and near-IR, especially those from SOLSPEC (Thuillier et al. 2003), provide an absolute temperature scale. Because these absolutely calibrated observations used for the models were obtained at shorter wavelengths (e.g., maximum wavelength from Thullier et al. is 2.4 μm), the computed spectral irradiance in the 3.7 μm band relies on the physical model of the solar atmosphere

derived from those observations and knowledge of absorption and emission radiative coefficients in the solar atmosphere.

The emergent irradiance spectrum from model C is computed at 1 AU in the manner described by Fontenla et al. (1999, 2006, as implemented in the Solar Radiation Physical Modeling system). The SRPM calculations show that the 3.7 μm continuum irradiance originates in photospheric layers with gas pressures between 0.57 $x10^5$ and 1.08$x10^5$ dyne cm^{-2} (heights from about 10 to 100 km above the $\tau_{500\,nm}$=1 level, and temperatures in the range 5480 to 6310 K), and that these layers encompass the significant formation of emitted radiance at all positions on the solar disk. The irradiance spectrum at 3.7 μm consists of a predominant continuum with a number of weak CO and OH molecular lines (only a few which are significant). Atomic lines of O, N, S, and C are also present but are not significant for the broadband calculations discussed in later sections. The lines we compute are evident in **Fig. 1** at sub-angstrom resolution, but due to a lack of reliable atomic data our calculated spectrum may contain a few less lines than the actual solar spectrum. However, the overall effects of the lines are small and only at longer wavelengths (about 4.295 μm, outside the band we consider) do CO bands become strong enough to produce a significant reduction in the broadband irradiance.

The main atomic parameter in the 3.7 μm band is the free-free opacity of the negative ion of Hydrogen. Fontenla, Balasubramanian & Harder (2006b) updated older estimates used in Fontenla et al. (2006) to the values published by Bell and Berrington (1987) and this produced some changes to the infrared intensities computed by SRPM. These opacity values are now thought to be accurate to within 2% (John 1988) which, taking into account the temperature gradient in the region of continuum formation, would result in about a 0.5% irradiance error.

However, the SRPM computed irradiance spectrum is 2.2% below Thuillier et al. (2003) at their longest measured wavelength (2.40 μm). This suggests that the 3.7 μm irradiance may be similarly underestimated in our calculations by perhaps 2%. Such an error is higher than what is estimated from the atomic data uncertainty but well within the combined error of the atomic data plus observations (~2% according to Thuillier 2003).

The Fontenla et al. (2006) models considered irradiance changes related to the solar activity cycle and rotation. Using the methods described by Fontenla and Harder (2005), it was found that the variations in solar irradiance in the 3.7 μm spectral region due to solar activity were less than ~0.5% of the quiet-Sun irradiance during the last 2 years. The magnitude of these variations are confirmed by the variability observed at visible and shorter IR wavelengths by the Spectral Irradiance Monitor (SIM) on board the Solar Radiation and Climate Experiment (SORCE) satellite (Harder et al. 2005, Rottman et al. 2005). The layers producing the 3.7 μm irradiance are just a bit shallower than those producing the visible irradiance at the continuum around 800 nm, and the observed and modeled irradiance variations are close to what is observed at that wavelength. Consequently, the model estimated variability at 3.7 μm is believed to be close to the real variability. These irradiance variations are relatively small compared with an uncertainty of about 2% in the overall value, which as explained above, is due to combined uncertainties in the available spectral irradiance observations and atomic data.

b. Model spectrum and comparisons with other data sets

Spectral irradiance from Fontenla et al. (2006) is plotted in **Fig. 1**. Line features are evident, especially around 4.05 μm, though they are relatively insignifi-

cant compared to continuum emission. All subsequent calculations use a reduced resolution form of the high-spectral resolution model output shown in the figure (convolution of the high resolution data with a 1 nm FWHM filter).

The irradiance curve of **Fig. 1** is well-approximated over the spectral range 3.40 – 4.15 μm (mean absolute deviation of 0.029 W-m^{-2}-μm^{-1}, or about 0.3 % relative) by the following quadratic function:

$$F_0(\lambda) = 157.91 - 66.34\,\lambda + 7.265\,\lambda^2 , \tag{4}$$

with λ in μm and $F_0(\lambda)$ in W-m^{-2}-μm^{-1}. Writing Eq. 4 in terms of wavenumber gives

$$F_0(\nu) = \frac{157.91\times10^4}{\nu^2} - \frac{66.34\times10^8}{\nu^3} + \frac{7.265\times10^{12}}{\nu^4} , \tag{5}$$

with ν in cm^{-1} and $F_0(\nu)$ in W-m^{-2}-(cm^{-1})$^{-1}$. As discussed in the next section, these analytic fits give band-averaged irradiances to about the 0.1% level or better relative to the actual Fontenla et al. spectrum. Brightness temperature is approximately linear across the spectral range (plot not shown) and can be accurately fit (4.3 K mean absolute deviation over the range 3.40-4.15 μm) by

$$T_B(\lambda) = 6533.6 - 229.6\,\lambda , \tag{6}$$

with λ in μm and T_B in K.

Plots of the data sets discussed in Section 2 are also shown in **Fig. 1**. As a reminder, other than the Kurucz (1995) spectrum, these historical data are observational, though all except Thekaedara (1974) are derived from disk center radiance measurements. The Thekaekara irradiance is uniformly larger than all other

datasets except at the shorter wavelengths where values are roughly the same as the Fontenla et al. (2006) and Kurucz spectrum. The Fontenla et al. and Kurucz spectra generally give irradiances within a couple of percent of each other, though the latter model shows more significant line features in the center of the 3.7 μm band. There is insufficient documentation on the Kurucz (1995) solar model and atomic and molecular data sources to compare with those used in our calculations. The Whehrli (1985) spectrum is biased high compared to the Kontratyev et al. (1965) and Murcray et al. (1964) data points, despite the fact that these data were the ultimate source for the Smith and Gottlieb (1974) fits adopted by Whehrli; however as noted in the Section 2, the limb darkening curve used by Smith and Gotlieb to convert these data to irradiance is not likely the same as the curve used by Pierce and Allen (1977) whose tabular values are shown in **Fig. 1**.

c. Instrument-specific sensitivity to the irradiance spectrum

Uncertainty in inferring the bi-directional reflectance from a 3.7 μm channel observation is dependent on the uncertainty in the instrument spectral response function, the solar irradiance spectrum, and the instrument's radiance calibration uncertainty (Eq. 1).

The relative spectral response functions for the 3.7 μm channel for four of the ten AVHRR instruments considered in this study, and the two MODIS instruments, are shown in **Fig. 2**. The Fontenla and Thekaekara spectral irradiance data (from **Fig. 1**) are also shown. The calculated bandpass and central wavelength in micrometers for both MODIS and all ten AVHRR instruments is given in **Table 1**. The two MODIS response functions are very similar while there is wide variation in the AVHRR channel characteristics (differences in central wavelength of over 90 nm between NOAA-12 and NOAA-15). All response functions are based

on pre-launch measurements, with the exception of NOAA-16 which flew the first AVHRR instrument to be characterized using a new automated spectral response function system with high spectral resolution capability. It was discovered that there had been a problem with the NOAA-16 AVHRR measurement setup after the satellite had been launched. Since an end-to-end spectral response measurement was no longer possible, a piecewise response function was calculated from each optical path component. This piecewise calculation is currently preferred over the original measurement (J. Sullivan, NOAA NESDIS, private communication).

While AVHRR and MODIS instruments are both filter radiometers, MODIS interference filters are made with a more stable ion-assisted deposition process (Montgomery et al. 2000). Further, MODIS has an onboard calibration source to monitor in-orbit changes in the channel center for spectral channels from the visible up to 2.1 μm (the Spectral Radiometric Calibration Assembly, Montgomery et al.) and no significant spectral shifts have been observed in these channels for either MODIS instrument (e.g., less than 0.2 nm for shortwave infrared channels, Xiong et al. 2005a). While 3.7 μm spectral stability cannot be monitored in-orbit, performance similar to the shorter wavelength channels is expected.

The differences in filter location and bandpass seen in **Fig. 2** result in substantial differences in the calculated average solar spectral irradiance over the channel (Eq. 2); such calculations for each instrument are given in **Tables 2a, 2b** for the Fontenla (2006), Thekaekara (1974), and Kurucz (1995) spectra. In the calculations, we integrated between the 0.02 relative spectral response function points. No attempt was made to account for low-level out-of-band responses. This includes the purported 4.2 μm spectral leak into the 3.7 μm channel of AVHRR NOAA-16 (A. Heidinger, NOAA NESDIS, private communication); this

leak is unlikely to have any significant impact due to Earth atmospheric CO_2 absorption. Regardless, out-of-band responses would in practice best be handled separately in radiative transfer calculations due to spectrally varying cloud and surface properties. The differences in channel-averaged irradiances from **Table 2a** relative to the Fontenla spectrum are given by the first pair of data columns in **Table 3**. As an example, for the MODIS Terra response function, use of the Thekaekara data results in an averaged spectral irradiance 3.85% larger than that obtained from Fontenla and 5.45% larger than use of the Kurucz spectrum. Similar values are found in the second pair of columns in **Table 3** where the irradiance differences have been given in terms of solar reflectance (Eqs. 1, 2). Note that the difference in the average irradiance between the two MODIS instruments is less that 0.5%, regardless of the irradiance spectrum used, while AVHRR differences can be in excess of 6% (NOAA-12 vs. NOAA-15).

For context, the calibration of MODIS solar bands used for cloud retrieval algorithms (visible through the 2.1 μm band) is derived from an onboard solar diffuser; including transfer of the diffuser calibration to the onboard diffuser observation, uncertainty is less than 2% for most solar bands (Xiong et al. 2005b). Instrument-specific uncertainties related to the 3.7 μm characterization of onboard blackbody calibration sources and their transfer need to be added appropriately to the numbers in **Table 3** (e.g., addition of variances assuming zero correlation) to provide an overall reflectance measurement uncertainty. The total RMS onboard radiance calibration uncertainty for the MODIS 3.7 μm channel (referred to as band number 20) has been evaluated to be less than 0.7% over a wide rand of radiances for both Terra and Aqua instruments (Xiong et al. 2005b). Therefore, for MODIS, the solar irradiance uncertainties of **Table 3** dominate the radiometric and spectral uncertainties and thus also dominate the reflectance calculation

uncertainty. Issues related to AVHRR thermal channel radiometric uncertainty and stability are discussed by Trishchenko (2002) and Trishchenko et al. (2002).

We used the analytic fits derived in the last section (Eqs. 4, 5) as a substitute for the Fontenla et al. (2006) irradiance spectrum and re-calculated the band-averaged irradiances in Tables 2a, 2b. For the twelve AVHRR and MODIS instruments in those tables, the band-averaged solar irradiance derived from Eqs. 4, 5 was not more than 0.1% different than those derived directly from the Fontenla et al. spectrum, with the exception of the NOAA-15 AVHRR which showed a 0.12% difference. For the MODIS instruments, the differences were better than 0.01%. Thus the equations provide band-averaged irradiances to a precision that is about a factor of 20 (or more) better than the estimated accuracy of the Fontenla et al. spectrum in this region (2% relative) and similarly smaller than the differences between the irradiance data sets compared in Table 3. As such, Eqs. 4 and 5 can be used for typical spectroradiometer 3.7 μm bandpass calculations without incurring any significant error in retrievals (see next section for cloud retrieval error context); exceptions would include narrowband spectrometers in the CO line portion of the solar atmosphere spectrum (Fig. 1).

d. Cloud retrieval sensitivity

The significance of the reflectance differences in **Table 3** for cloud retrieval applications was empirically investigated using a Terra MODIS data granule of coastal Chile and Peru that has been previously discussed (Platnick et al. 2003). The granule (5 minutes of data) includes a variety of cloud types, including marine boundary layer water clouds, cirrus over land and ocean, and convective ice and water clouds over the Amazon basin. Retrievals were obtained from the operational MODIS Terra cloud product (MOD06) Collection 5 processing stream

code, that includes separate effective retrievals derived from 3.7 μm MODIS observations (as well as size retrievals derived from 1.6 and 2.1 μm observations, separately and in combination). Histograms of liquid water and ice cloud effective radius retrievals for the data granule are shown in **Fig. 3** using two different values for the 3.7 μm MODIS channel-averaged spectral irradiance (a 5% difference). The 11.34 $W\text{-}m^{-2}\text{-}\mu m^{-1}$ value corresponds to the average of the MODIS Terra and Aqua instrument irradiances using the Thekaekara (1974) data set. The smaller irradiance (10.77 $W\text{-}m^{-2}\text{-}\mu m^{-1}$) is comparable to the instrument averages using either Fontenla (2006) or Kurucz (1995). For liquid water clouds, the difference in the mean value of the retrieved effective radius over the data granule is 0.50 μm (≈4.5%); for ice clouds, the difference is 0.71 μm (≈6.5%).

To place these differences in context, the 3.7 μm effective radius retrieval uncertainty for these MODIS retrievals was calculated assuming the spectral irradiance is known exactly, but including the following set of error sources contributing to the reflected signal: instrument calibration and forward model uncertainty (5%), surface spectral albedo uncertainty (15%), above-cloud column water vapor amount derived from model analysis and MODIS cloud-top pressure retrievals for use in spectral atmospheric corrections (20%). Each error source is assumed uncorrelated. Note that the uncertainty analysis does not include errors in the estimation of cloud-top temperature, surface temperature, and atmospheric state that are required to account for the 3.7 μm emission component. The retrieval uncertainty is a function of effective radius and cloud optical thickness, as well as surface type and atmospheric state, and as such, is difficult to summarize succinctly (Platnick et al. 2004). However, for comparison with the granule-averaged means of **Fig. 3**, mean 3.7 μm effective radius relative uncertainties are 5.2% and 6.4% for liquid water and ice clouds, respectively. Therefore, in this ex-

ample, the uncertainty in the retrieved effective radius due to a 5% irradiance uncertainty is of the same order as other fundamental reflectance error sources.

4. Discussion

Despite the widespread presence of a 3.7μm atmospheric window channel on present-day and planned satellite imagers, the absolute top-of-atmosphere solar spectral irradiance in the band, which is required for daytime quantitative use, is limited to a single aircraft field campaign (Thekaekara et al. 1969, Thekaekara 1974). This sole observational irradiance data set was discussed, along with a survey of published radiance observations, and compared with historical synthetic data sets and the new solar models of Fontenla et al. (2006, 2006b). Channel-averaged spectral irradiances using the various data sets were calculated for laboratory-derived AVHRR and MODIS instrument spectral response functions. Depending on the particular instrument, the observations reported by Thekaekara (1974) give averaged irradiances from about +3.2% to +4.1% greater than the quiet-Sun Fontenla et al. spectrum; the Kurucz spectra gives channel-averaged irradiances about -1.2% to -1.5% smaller than Fontenla et al. The new Fontenla et al. irradiance spectrum is expected to have a 2% uncertainty in the 3.7 μm region.

The consequences on cloud microphysical retrievals from uncertainty in the 3.7 μm band solar irradiance was examined for a MODIS data granule consisting of a variety of liquid and ice clouds over both ocean and land. Using a representative channel-averaged solar irradiance uncertainty of 5%, based on this study's comparisons of observational and modeled irradiances, averaged retrieved effective radius uncertainties averaged for all pixels in the data granule were 4.5% and 6.5% for liquid water and ice clouds, respectively. This is comparable to re-

trieval uncertainties due to other error sources that fundamentally impact the inference of cloud-top reflectance in the band. Retrieval uncertainties from errors in estimating emitted radiance in the channels were not considered.

The quiet-Sun irradiance spectrum from Fontenla et al. used in this study (as implemented in the Solar Radiation Physical Modeling (SRPM) system) is planned for inclusion in the upcoming MODTRAN5 release. In the meantime, analytic fits to the Fontenla et al. spectral irradiance and brightness temperature from 3.4-4.15 μm have been provided (Eqs. 4, 5, and 6). For the AVHRR and MODIS instruments of Tables 2, the irradiance fits provide band-averaged irradiance precision in the 3.7 μm channels to about the 0.1% level or better.

While the relative agreement between modeled spectra and Thekaekara (1974) in the 3.7 um band is reassuring, new absolute spectral irradiance observations in the band are sorely needed to augment the sole available observations reported by Thekaekara.

Acknowledgments. This research was supported in part by the NASA Radiation Science Program under grant 621-30-92 (SP); JMF was supported by contract NAS5-97045 at the University of Colorado. We are grateful to Drs. Andrew Heidinger at NOAA NESDIS and Xiaoxiong ("Jack") Xiong at the NASA Goddard Space Flight Center for their input, and anonymous reviewers for helpful comments and suggestions.

References

Ackerman, S. A., K. I. Strabala, W. P. Menzel, R. A. Frey, C. C. Moeller, and L. E. Gumley, 1998: Discriminating clear-sky from clouds with MODIS. *J. Geophys. Res.*, **103**, 32141-32158.

American Society for Testing and Materials, *Standard Extraterrestrial Spectrum Reference E-490*, http://www.astm.org.

Aminou, D. M. A., 2002: MSG's SEVIRI instrument. *European Space Agency Bulletin*, **111**, 15-17.

Arking, A., and J. D. Childs, 1985: Retrieval of cloud cover parameters from multispectral satellite images. *J. Clim. Appl. Meteor.*, **24**, 322-333.

Barnes, W. L., T. S. Pagano, and V. V. Salomonson, 1998: Prelaunch characteristics of the Moderate Resolution Imaging Spectroradiometer (MODIS) on EOS-AM1. *IEEE Trans. Geosci. Remote Sensing*, **30**, 2–27.

Barnes, R. A., W. L. Barnes, C.-H. Lyu, and J. M. Gales, 2000: An Overview of the Visible and Infrared Scanner Radiometric Calibration Algorithm. *J. Atmos. and Oceanic Tech.*, **17**, 395–405.

Bell, K. L., and K. A. Berrington, 1987: Free-free absorption coefficient of the negative hydrogen ion. *J. Phys. B*, **20**, 801-806.

Berk, A., G. P. Anderson, P. K. Acharya, M. L. Hoke, J. H. Chetwynd, L. S. Bernstein, E. L. Shuttle, M. W. Matthew, and S. M. Adler-Golden, 2003: *MODTRAN4 Version 3 Revision 1 User's Manual*. Air Force Res. Lab., Hanscom Air Force Base.

Elterman, L., and R. B. Toolin, *Handbook of Geophysics and Space Environments*, S. L. Valley, Ed., McGraw-Hill, 1965.

Farmer, C. B., 1994: The ATMOS solar atlas. *Infrared Solar Phys. IAU Symposia*, **154**, 511-521.

Fontenla, J. M., O. R. White, P. A. Fox, E. H. Avrett, and R. L. Kurucz, 1999: Calculation of solar irradiances. I. Synthesis of the solar spectrum. *Astrophys. J.*,

518, 480-499.

Fontenla, J. M, and J. W. Harder, 2005: Physical modeling of spectral irradiance variations. *Mem. S. A. I.*, **76**, 826-833.

Fontenla, J. M., E. Avrett, G. Thuillier, and J. Harder, 2006: Semiempirical models of the solar atmosphere. I. The quiet- and active sun photosphere at moderate resolution. *Astrophys. J.*, **639**, 441-458.

Fontenla, J. M., K. S. Balasubramanian, and J. W. Harder, 2006b: Semiempirical models of the solar atmosphere. II. The quiet-Sun low-chromosphere at moderate resolution, (in preparation).

Han, Q., W. B. Rossow, and A. A. Lacis, 1994: Near-global survey of effective droplet radii in liquid water clouds using ISCCP data. *J. Climate*, **7**, 465-497.

Harder, J. W., J. M. Fontenla, O. White, G. Rottman, and T. Woods, 2005: Solar spectral irradiance variability comparisons of the SORCE SIM instrument with monitors of solar activity and spectral synthesis. *Mem.S.A.I.*, **76**, 735-742.

Heidinger, A. K., V. Rao, A. Dean, and C. Dean, 2002: Using MODIS to estimate cloud contamination of the AVHRR data record. *J. Atmos. Oceanic Tech.*, **19**, 586-601.

John, T. L., 1988: Continuous absorption by the negative hydrogen ion reconsidered. *Astron. Astrophys.*, **193**, 189-192.

Justice, C. O, L. Giglio, S. Korontzi, J. Owens, J. T. Morisette, D. Roy, J. Descloitres, S. Alleaume, F. Petitcolin, and Y. Kaufman, 2002: The MODIS fire products. *Remote Sens. Env.*, **83**, 244-262.

Kaufman, Y. J., C. J. Tucker and I. Fung, 1990: Remote sensing of biomass burning in the tropics, *J. Geophys. Res.*, **95**, 9927-9939.

King, M. D., W. P. Menzel, P. S. Grant, J. S. Myers, G. T. Arnold, S. Platnick, L. E. Gumley, S. C. Tsay, C. C. Moeller, M. Fitzgerald, K. S. Brown, and F. G. Osterwisch, 1996: **A**irborne Scanning Spectrometer for Remote Sensing of

Cloud, Aerosol, Water Vapor, and Surface Properties. *J. Atmos. and Oceanic Tech.*, **13**, 777-794.

Kondratyev, K. Y., S. D. Andreev, I. Y. Badinov, V. S. Grishechkin, and L. V. Popova, 1965: Atmospheric optics investigations on Mt. Elbrus. *Appl. Opt.*, **4**, 1069-1076.

Koutchmy, S., and R. Peyturaux, 1970: Study of the solar continuum in the intermediate infra-red spectral range 3.5-24.4 μ. *Astron. Astrophys.*, **5**, 470-487.

Kurucz, R.L., 1995: The Solar Irradiance by Computation. *Proceedings of the 17th Annual Review Conference on Atmospheric Transmission Models*, eds. G. P. Anderson, R. H. Picard, and J. H. Chetwynd, PL/-TR-95-2060, Special Reports, No. 274, Pl. 332, Phillips Laboratory Geophysics Directorate, MA, May 1995.

Lee, T. E., S. D. Miller, F. J. Turk, C. Schueler, R. Julian, S. Deyo, P. Dills, and S. Wang, 2006: The NPOESS VIIRS day/night visible sensor. *Bull. Amer. Meteor. Soc.*, **87**, 191-199.

Livingston, W., and L. Wallace, 1991: An atlas of the solar spectrum in the infrared from 1.1 to 5.4 μm, *National Solar Observatory Technical Report*, 91-001.

Maltby, P., E. H. Avrett, M. Carlsson, O. Kjeldseth-Moe, R. L. Kurucz, and R. Loeser, 1986: A new sunspot umbral model and its variation with the solar cycle. *Astrophys. J.*, **306**, 284-303.

Montgomery, H., N. Che, K. Parker, and J. Bower, 2000: The algorithm for MODIS wavelength on-orbit calibration using the SRCA. *IEEE Trans. Geosci. Rem. Sens.*, **38**, 877-884.

Minnis et al., 1995: Cloud optical property retrieval (sub-system 4.3). Cloud analyses and radiance inversions (subsystem 4), Vol. III, Clouds and the Earth's Radiant Energy System (CERES) algorithm theoretical basis document, *NASA Ref. Publ.* 1376, **3**, 135–176.

Murcray, F. H., D. G. Murcray, and W. J. Williams, 1964: The spectral radiance of

the sun from 4 micrometer to 5 micrometer. *Appl. Opt.*, **3**, 1373-1377.

Nakajima, T. Y., T. Nakajima, M. Nakajima, H. Fukushima, M. Kuji, A. Uchiyama, and M. Kishino, 1998: Optimization of the Advanced Earth Observing Satellite II Global Imager channels by use of radiative transfer calculations. *Appl. Opt.*, **37**, 3149-3163.

Pavolonis, M. J., A. K. Heidinger, and T. Uttal, 2005: Daytime global cloud typing from AVHRR and VIIRS: Algorithm description, validation, and comparisons. *J. Appl. Meteo.*, **44**, 804-826.

Pierce, A. K., and R. G. Allen, 1977: The solar spectrum between .3 and 10 μm. *The Solar Output and its Variation*, O. R. White, Ed., Colorado Associated University Press, Boulder, 169-192.

Platnick, S., and S. Twomey, 1994: Determining the susceptibility of cloud albedo to changes in droplet concentrations with the Advanced Very High Resolution Radiometer. *J. Appl. Meteo.*, **33**, 334-347.

Platnick, S., M. D. King, S. A. Ackerman, W. P. Menzel, B. A. Baum, J. C. Riédi, and R. A. Frey, 2003: The MODIS cloud products: Algorithms and examples from Terra. *IEEE Trans. Geosci. Remote Sens.*, **41**, 459-473.

Platnick, S., R. Pincus, B. Wind, M. D. King, M. Gray, and P. Hubanks, 2004: An initial analysis of the pixel-level uncertainties in global MODIS cloud optical thickness and effective particle size retrievals. *Proc. of SPIE*, **5652**, 30-40.

Prins, E. M. and W.P. Menzel, 1992: Geostationary satellite detection of biomass burning in South America. *Int. J. Remote Sens.*, **13**, 2783-2799.

Rottman, G., J. Harder, J. Fontenla, T. Woods, O.R. White, and G. M. Lawrence, 2005: The spectral irradiance monitor (SIM): Early observations. *Solar Phys.*, **230**, 205-244.

Saunders, R.W., and K. T. Kriebel, 1988: An improved method for detecting clear sky and cloudy radiances from AVHRR data. *Int. J. Rem. Sens.*, **9**, 123-150.

Schmit, T. J., M. M. Gunshor, W. Paul Menzel, Jun Li, Scott Bachmeier, and James

J. Gurka, 2005: Introducing the Next-generation Advanced Baseline Imager (ABI) on GOES-R. *Bull. Amer. Meteor. Soc.*, **86**, 1079-1096.

Schwalb, A., 1978: *The TIROS-N/NOAA A-G satellite series*. NOAA Tech. Mem. NESS 95, 75 pp.

Scorer, R. S., 1986: Cloud Investigation by Satellite, Ellis Horwood, Chichester.

Scorer, R. S., 1989: Cloud reflectance in channel-3. *Int. J. Rem. Sens.*, **10**, 675-686.

Smith, E. V. P., and D. M.Gottlieb, 1974: Solar flux and its variation. *Space Sci. Rev.*, **16**, 771-802.

Thekaekara, M. P., R. Kruger, and C. H. Duncan, 1969: Solar irradiance measurements from a research aircraft. *Appl. Opt.*, **8**, 1713-1732.

Thekaekara, M. P., 1974: Extraterrestrial solar spectrum, 3000-6100 Å at 1- Å intervals. *Appl. Opt.*, **13**, 518-522.

Thuillier, G., M. Hersé, D. Labs, T. Foujols, W. Peetermans, D. Gillotay, P. C. Simon, and H. Mandel, 2003: The solar spectral irradiance from 200 to 2400 nm as measured by the SOLSPEC spectrometer from the Atlas and Eureca missions. *Solar Phys.*, **214**, 1-22.

Trishchenko, A. P., 2002: Removing unwanted fluctuations in the AVHRR thermal calibration data using robust techniques. *J. Atmos. Oceanic Tech.*, **19**, 1939-1954.

Trishchenko, A. P., G. Fedosejevs, Z. Li, and J. Cihlar, 2002: Trends and uncertainties in thermal calibration of AVHRR radiometers onboard NOAA-9 to NOAA-16. *J. Geophys. Res.*, **107 (D24)**, 4778, doi:10.1029/2002JD002353.

Trishchenko, A. P., 2006: Solar irradiance and effective brightness temperature for SWIR channels of the AVHRR/NOAA and GOES imagers. *J. Atmos. Oceanic Tech.*, **23**, 198-210.

Wehrli, C., 1985: Extraterrestrial solar spectrum. *Physikalisch-Meteorologisches Observatorium Davos and World Radiation Center*, pub. 615 (available from *ftp://ftp.pmodwrc.ch/pub/data/irradiance/spectral_irradiance*).

Xiong, X., N. Che, B. Guenther, W. L. Barnes, and V. V. Salomonson, 2005a: Five years of Terra MODIS On-orbit spectral calibration, *Proc. Of SPIE*, **5882**, doi: 10.1117/12.614090.

Xiong, X., J. Sun, A. Wu, K.-F. Chiang, J. Esposito, and W. Barnes, 2005b: Terra and Aqua MODIS calibration algorithms and uncertainty analysis, *Proc. Of SPIE*, **5978**, doi: 10.1117/12.627631.

Figure Captions

FIG. 1. Plot of selected solar spectral irradiance datasets discussed in the text for the 3.7 μm band spectral region. Data points for Kondratyev et al. and Murcray et al. were taken from Pierce and Allen (1977).

FIG. 2. 3.7 μm channel relative spectral response functions for the two MODIS instruments (NASA Terra and Aqua spacecrafts) and a subset of the AVHRR instruments (NOAA polar orbiting platforms 9, 14, 15, and 16) used for channel-averaged irradiance calculations. The solar spectral irradiance from Fontenla et al. (2006) and Thekaekara (1974), taken from Fig. 1, is also shown.

FIG. 3. Frequency histogram for liquid water and ice cloud retrievals from a MODIS Terra data granule (see text for details) using two different values for the channel-averaged spectral irradiance. The mean effective radius for the retrievals is given in parenthesis.

Table 1. The spectral response function Full-Width-Half-Maximum (FWHM) bandpass and central wavelength (defined as the average of the two FWHM wavelengths) for AVHRR and MODIS 3.7 μm channels used in this study.

Instrument/ Platform	Central Wavelength (μm)	Bandpass (μm)
AVHRR N7	3.741	0.411
AVHRR N9	3.733	0.410
AVHRR N10	3.763	0.375
AVHRR N11	3.750	0.400
AVHRR N12	3.800	0.400
AVHRR N14	3.788	0.425
AVHRR N15	3.708	0.322
AVHRR N16	3.724	0.326
AVHRR N17	3.761	0.385
AVHRR N18	3.768	0.385
MODIS Terra	3.792	0.190
MODIS Aqua	3.785	0.189

Table 2a. Channel-averaged solar spectral irradiance for AVHRR and MODIS 3.7 μm instrument channels, for three spectral irradiance data sets.

Instrument/ Platform	Band-Averaged Solar Spectral Irradiance ($W\text{-}m^{-2}\text{-}\mu m^{-1}$) Solar Irradiance Dataset		
	Fontenla et al. (2006)	Thekaekara (1974)	Kurucz (1995)
AVHRR N7	11.573	11.957	11.429
AVHRR N9	11.671	12.043	11.528
AVHRR N10	11.360	11.771	11.216
AVHRR N11	11.543	11.930	11.400
AVHRR N12	11.020	11.470	10.879
AVHRR N14	11.138	11.573	10.997
AVHRR N15	11.729	12.101	11.577
AVHRR N16	11.467	11.867	11.317
AVHRR N17	11.327	11.741	11.184
AVHRR N18	11.200	11.627	11.059
MODIS Terra	10.885	11.304	10.720
MODIS Aqua	10.974	11.386	10.807

Table 2b. Same as Table 2a but in wavenumber spectral density.

Instrument/ Platform	Band-Averaged Solar Spectral Irradiance ($W\text{-}m^{-2}\text{-}(cm^{-1})^{-1}$) Solar Irradiance Dataset		
	Fontenla et al. (2006)	Thekaekara (1974)	Kurucz (1995)
AVHRR N7	1.6096	1.6644	1.5895
AVHRR N9	1.6159	1.6710	1.5970
AVHRR N10	1.5890	1.6442	1.5681
AVHRR N11	1.6060	1.6586	1.5850
AVHRR N12	1.5655	1.6261	1.5454
AVHRR N14	1.5757	1.6335	1.5550
AVHRR N15	1.6189	1.6777	1.5963
AVHRR N16	1.6019	1.6606	1.5819
AVHRR N17	1.5929	1.6481	1.5724
AVHRR N18	1.5842	1.6395	1.5650
MODIS Terra	1.5607	1.5739	1.5384
MODIS Aqua	1.5666	1.5810	1.5432

Table 3. Difference in the 3.7 μm channel-averaged solar spectral irradiance and inferred solar reflectance relative to the Fontenla et al. (2006) data set, as derived from Table 2a.

Instrument/ Platform	Relative Difference (%) in Solar Irradiance vs. Fontenla Irradiance Dataset		Relative Difference (%) in Inferred Solar Reflectance vs. Fontenla Irradiance Dataset	
	Thekaekara (1974)	Kurucz (1995)	Thekaekara (1974)	Kurucz (1995)
AVHRR N7	3.32	-1.24	-3.21	1.26
AVHRR N9	3.19	-1.23	-3.09	1.24
AVHRR N10	3.62	-1.27	-3.49	1.28
AVHRR N11	3.35	-1.24	-3.24	1.25
AVHRR N12	4.08	-1.28	-3.92	1.30
AVHRR N14	3.91	-1.27	-3.76	1.28
AVHRR N15	3.17	-1.30	-3.07	1.31
AVHRR N16	3.49	-1.31	-3.37	1.33
AVHRR N17	3.65	-1.26	-3.53	1.28
AVHRR N18	3.81	-1.26	-3.67	1.27
MODIS Terra	3.85	-1.52	-3.71	1.54
MODIS Aqua	3.75	-1.52	-3.62	1.55

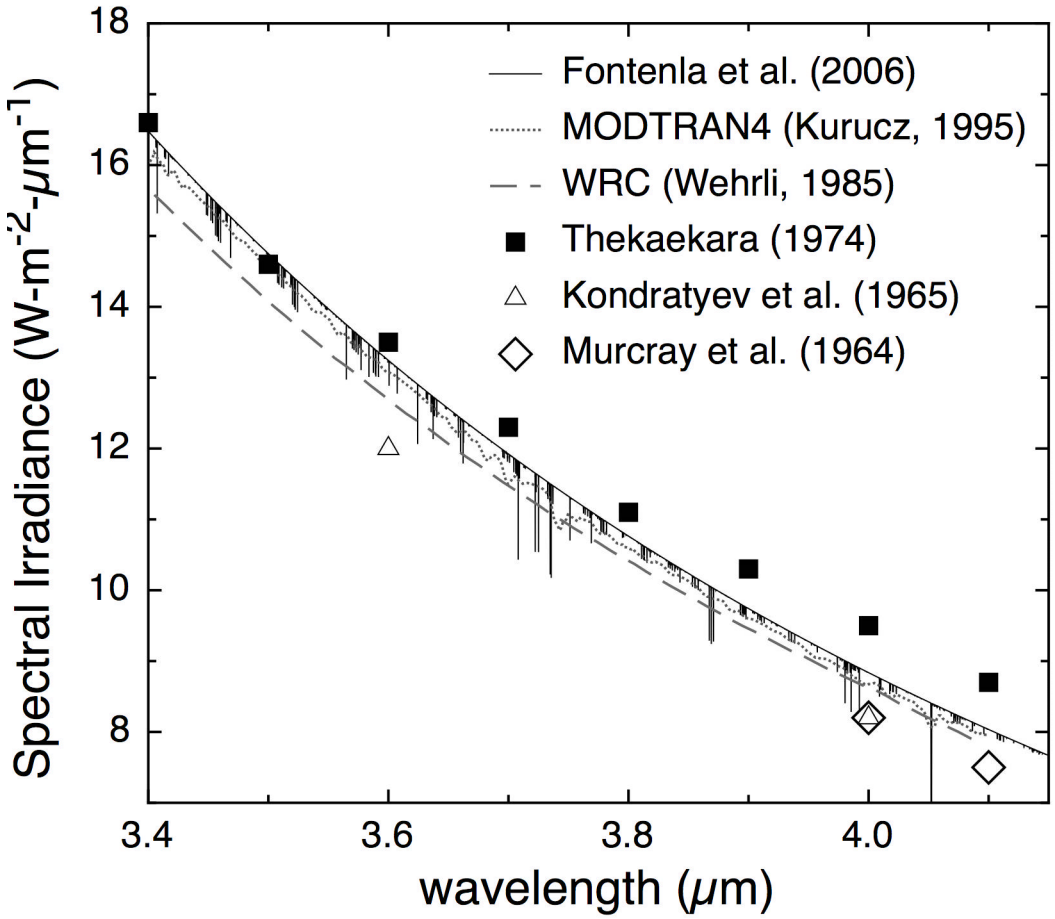

FIG. 1. Plot of selected solar spectral irradiance datasets discussed in the text for the 3.7 μm band spectral region. Data points for Kondratyev et al. and Murcray et al. were taken from Pierce and Allen (1977).

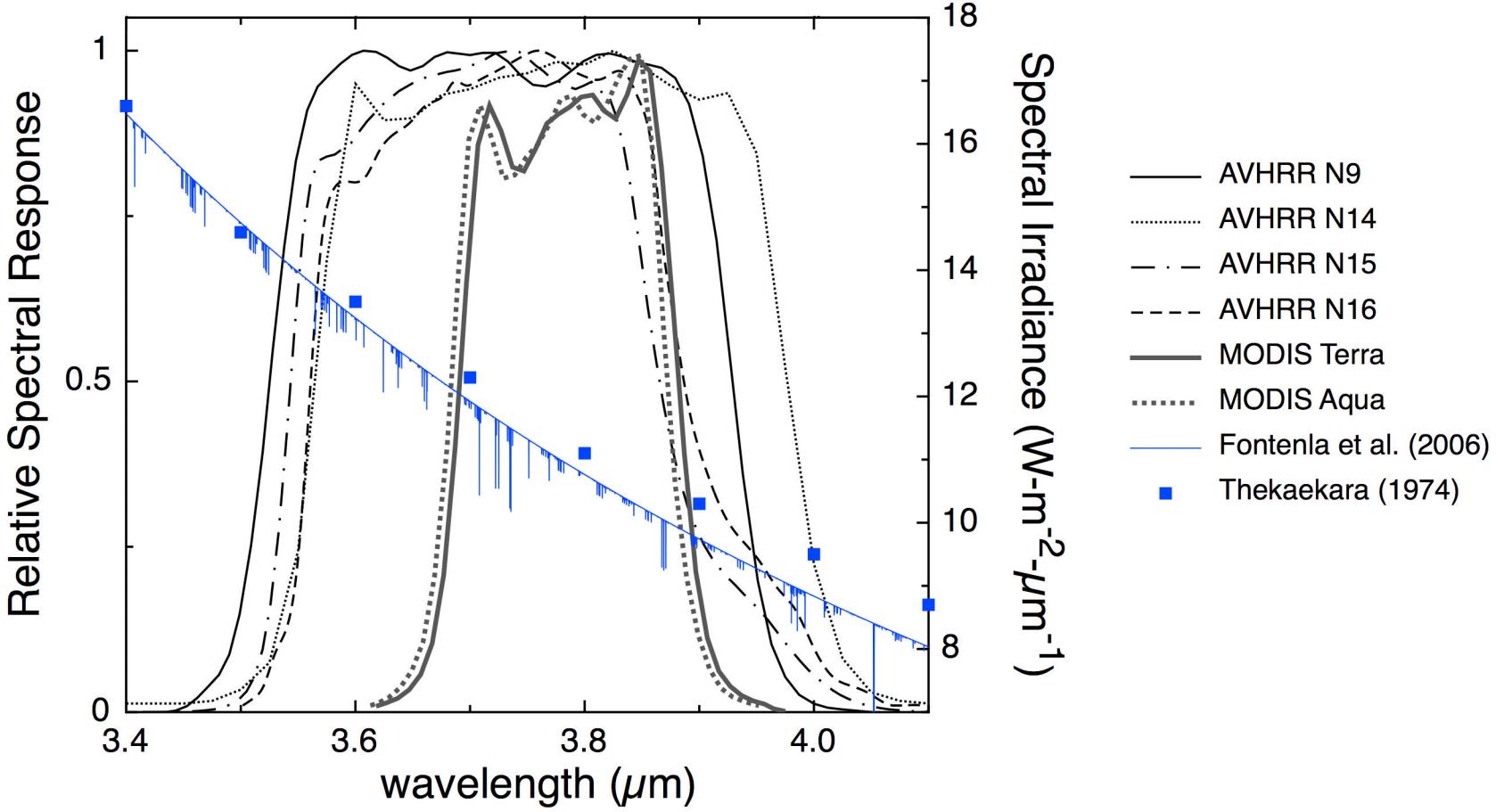

FIG. 2. 3.7 μm channel relative spectral response functions for the two MODIS instruments (NASA Terra and Aqua spacecrafts) and a subset of the AVHRR instruments (NOAA polar orbiting platforms 9, 14, 15, and 16) used for channel-averaged irradiance calculations. The solar spectral irradiance from Fontenla et al. (2006) and Thekaekara (1974), taken from Fig. 1, is also shown.

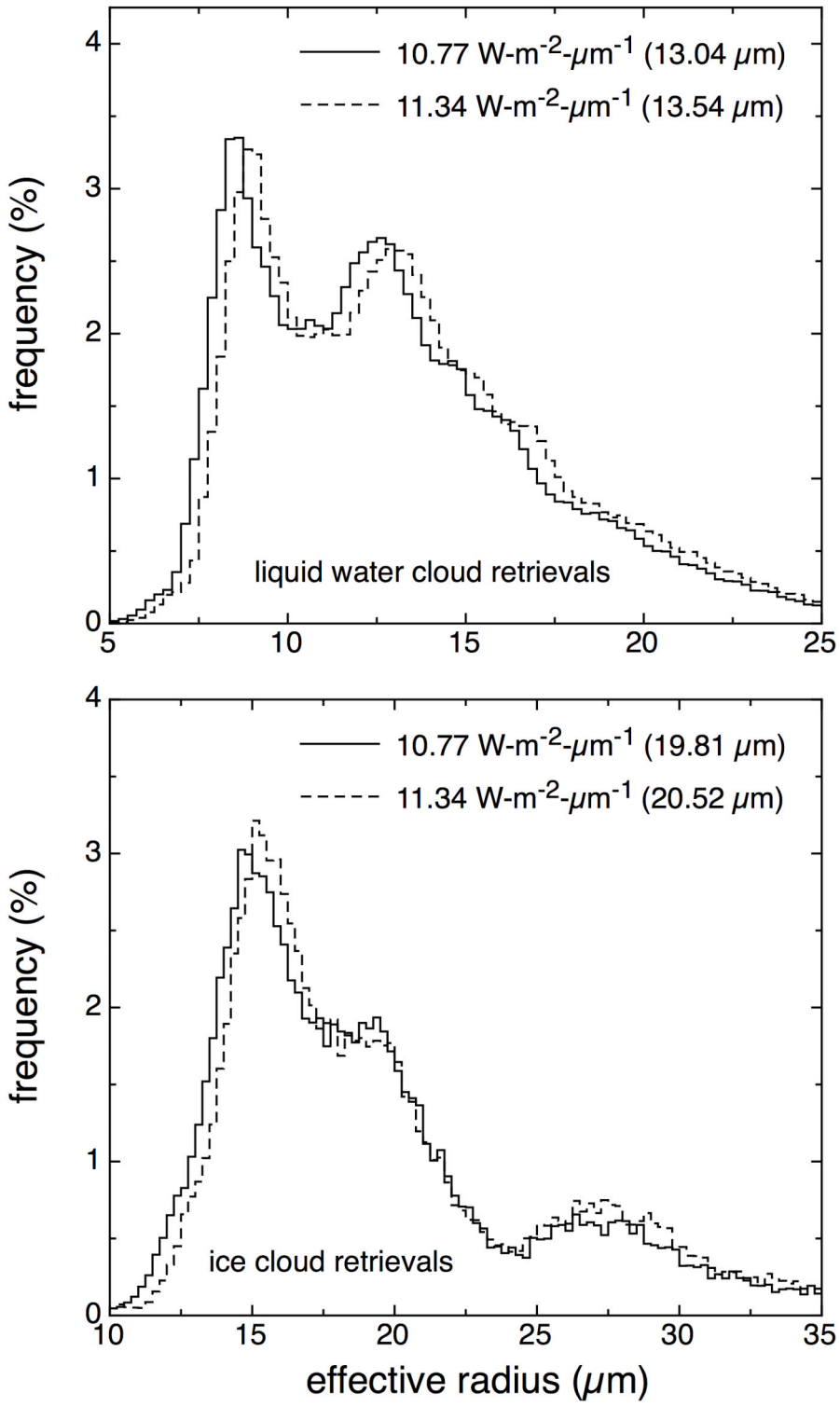

FIG. 3. Frequency histogram for liquid water and ice cloud retrievals from a MODIS Terra data granule (see text for details) using two different values for the channel-averaged spectral irradiance. The mean effective radius for the retrievals is given in parenthesis.